A Flexible Valve Based Piezoelectric Pump for High Viscosity Cooling Liquid Transportation

LI Kai[1], *LIU Jiaming*[2], *ZHANG Quan*[3], *ZHANG Jianhui*[4], *HUANG Jun*[2*], *WANG Yuan*[5]

1. New Combined Power R&D Center, Shaanxi Province Aerospace and Astronautics Propulsion Research Institute Co. Ltd., Xi'an 710003, P.R. China;
2. Research Center of Fluid Machinery Engineering and Technology, Jiangsu University, Zhenjiang 212013, P. R. China;
3. School of Mechatronic Engineering and Automation, Shanghai University, Shanghai 200072, P. R. China;
4. College of Mechanical and Electrical Engineering, Guangzhou University, Guangzhou 510006, P. R. China;
5. College of Communication Engineering, Army Engineering University of PLA, Nanjing 210007, P. R. China

(Received 22 March 2021; revised 11 April 2021; accepted 10 June 2021)

Abstract: A piezoelectric pump with flexible valve has been developed to pump high viscosity cooling liquid in the nanosats thermal control system. The structure of the flexible valve is designed according to the characteristics of the human aortic shape with the aim to simulate the bionic pumping function of the human heart. Dynamic stress-strain features of the flexible valve are analyzed by the finite element method, and the results show that the proposed flexible valve is suitable and functional for the piezoelectric pump. Then the cylinder and diffuser/nozzle piezoelectric pumps based on flexible valves have been developed and fabricated. Experimental results of the output performance indicate that the maximum flow rate of the cylinder piezoelectric pump with flexible valve is 15.38 mL/min, 170.77% higher than the diffuser/nozzle piezoelectric pump with flexible valve. The ability of the cylinder piezoelectric pump with flexible valve for transmitting high viscosity liquid has been validated. The piezoelectric pump with flexible valve has potential applications in the nanosats thermal control system.

Key words: piezoelectric pump; high viscosity liquid; flexible valve; cut-off performance; pumping performance

CLC number: TH38 **Document code:** A **Article ID:** 1005-1120(2021)06-0993-10

0 Introduction

With the rapid development of nanosats, the heat flux density of the nanosat load is rising, putting higher demands on the thermal control system incorporated on nanosats[1-3]. The micropump, as the driving source of the active thermal control system, is critical in heat regulation and thermal management control[4-5]. Micropumps are divided into many groups based on their actuation mechanism[6], including vane[7-8], electrostatic[9], piezoelectric[10-11], thermo-pneumatic[12], electromagnetic[13], and shape memory alloy micropumps[14]. Among them, piezoelectric micropumps are the most common ones, with various advantages such as small scale, high durability, strong actuation power, and no magnetic effect.

According to the structure with or without a valve, the piezoelectric pump can be divided into two types, i. e., valve pump and valveless pump. To replace the function of valves, diffuse/nozzle, Y-shape channel, vortex diode, etc. are widely used in the valveless piezo-pump[15-21]. Inspired by female mosquitoes drinking liquid with different viscosities, Lee et al.[22] proposed a bionic serially connected valveless piezoelectric micropump. The pump featured the ability to transfer the liquid with the viscosity up to 2.28 cP, with a maximum output flow rate of more than 400 μL/min. Since there is no moving valve, the valveless piezoelectric pump has the advantages of simple structure and high reliability, but it also has the common problems of large output pulsation and low output flow rate. Therefore, the output performance of the valveless

*Corresponding author, E-mail address: huangjun@ujs.edu.cn.

How to cite this article: LI Kai, LIU Jiaming, ZHANG Quan, et al. A flexible valve based piezoelectric pump for high viscosity cooling liquid transportation[J]. Transactions of Nanjing University of Aeronautics and Astronautics, 2021, 38(6): 993-1002.

http://dx.doi.org/10.16356/j.1005-1120.2021.06.010

piezoelectric pump is difficult to meet the thermal control requirements, and it is not suitable for the active thermal control system of nanosat.

Compared with the valveless piezoelectric pump, the output characteristics of the valve piezoelectric pump have the advantages of large output flow rate and small pulsation. Cantilever valve, wheel valve, and umbrella valve, etc. are widely used in valve piezoelectric pumps. Peng et al.[23] proposed a multi-chambers piezolectric pump with umbrella valves. The umbrella valve was made of silica gel, and the output flow of the pump reached 1 845 mL/min. Dong et al.[24] designed a single vibrator piezoelectric micropump integrating the wheel valve and the piezo-vibrator, with a maximum flow rate of 2 034.7 mL/min. However, frequent on/off actions can cause fatigue damage to the valve body, which may lead to valve body failure. Therefore, Huang et al. [25] designed a cymbal-shaped slotted valve to improve the deformation of the valve body and reduce the stress. But the cymbal-shaped slotted valve is curved shape and processed with metal materials, so it is difficult to manufacture and assemble. By referring to the structure of human heart valve, a flexible valve is proposed, and the piezoelectric pump with flexible valve is designed to reduce the stress of the valve and thus improve the reliability of piezoelectric micropumps.

The piezoelectric pump with flexible valve is proposed to transport cooling liquids with wide viscosity range. The dynamic stress-strain characteristic of the flexible valve is analyzed by the finite element method. And the prototype piezo-pumps are fabricated. The variations in flow rate of piezoelectric pumps are experimentally investigated with varying driving frequency and viscosity of the working fluid. The piezoelectric pump with flexible valve has tremendous potential applications in the thermal control system of nanosats.

1 Design and Working Principle

The structure of a flexible arterial valve is shown in Fig. 1. According to the structure of the aortic valve between the left ventricle of human heart and aorta, the flexible arterial valve consists of three flaps with the thickness of 0.8 mm and the width of 0.8 mm. The three flaps are spaced evenly every 120° to create a compact valve with a radius of 17 mm and a height of 4 mm. The ventral flap's design is covered by the intersection of an ellipsoid and a cylinder. Besides, the ellipsoid and cylinder parametric equations are shown as

$$\begin{cases} x = 18\sin\theta\cos\varphi & \frac{\pi}{2} \leqslant \theta \leqslant \pi \\ y = 18\sin\theta\sin\varphi & \\ z = 4\cos\theta & 0 \leqslant \varphi \leqslant \pi \end{cases} \tag{1}$$

$$\begin{cases} x = 18\sin\varphi & 0 \leqslant \varphi \leqslant 2\pi \\ y = 18\cos\varphi & -\infty \leqslant u \leqslant +\infty \\ z = u & \end{cases} \tag{2}$$

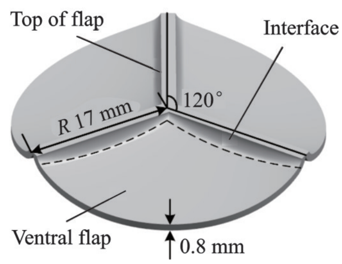

Fig.1 Structure of flexible arterial valve

The structure of a diffuser/nozzle piezoelectric pump with flexible valve is shown in Fig.2, which consists of a piezoelectric vibrator, a flexible arterial valve, and diffuser/nozzle channels. The structure of a cylinder piezoelectric pump with flexible valve is shown in Fig.3. The cylindrical channels are substituted for diffuser/nozzle channels.

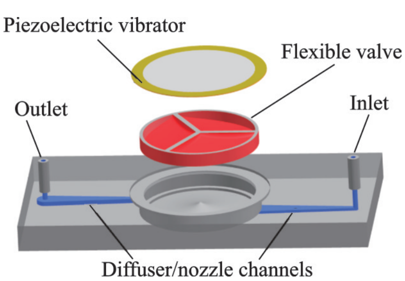

Fig.2 Structure of diffuser/nozzle piezoelectric pump with flexible valve

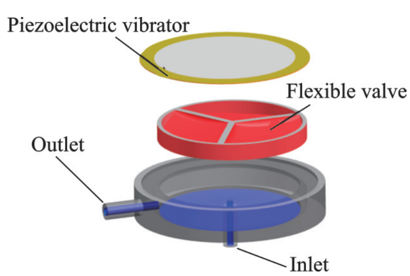

Fig.3 Structure of cylindrical piezoelectric pump with flexible valve

The working principle of the piezoelectric pump with flexible valve is demonstrated in Fig. 4. Driven by an AC signal, the piezo-vibrator generates reciprocating vibration. When the volume of the pump chamber expands, the external fluid is sucked into the pump chamber through the diffuser/nozzle channels due to the pressure difference. At this moment, the flexible valve is opened. This procedure is defined as the suction mode. When the volume of the pump chamber is constricted, the fluid in the pump cavity is forced out of the pump through the diffuser/nozzle channels. The flexible valve is closed. Such a procedure can be defined as the discharge mode.

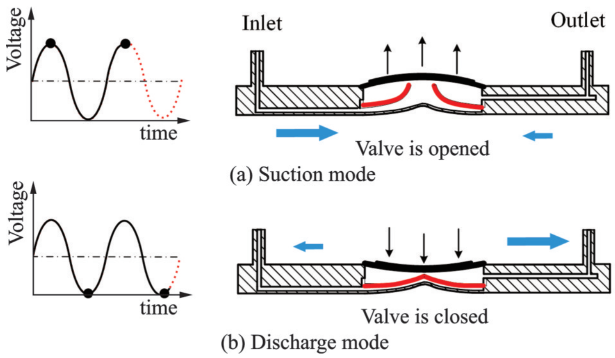

Fig.4 Working principle of piezo-pump

2 Numerical Simulation

The finite element method (FEM) is employed to calculate the forward and reverse displacements of the flexible valve under different pressures. The finite element model is shown in Fig.5. The model is imported into ANSYS multiphysics for calculation. The elastic materials with young's modulus of 3 MPa, Poisson's ratio of 0.45 and density of 1 200 kg/m^3 are defined as calculation objects. According to the design conditions of the piezoelectric pump, the instantaneous pressure load is set on the loading surface, and the function of the loads is shown as $p=150\cdot\sin(2\times 180\times 20\times t)$, where t is time and p the pressure in the vertical direction.

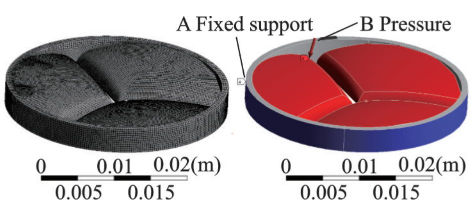

Fig.5 Finite element model of flexible valve

In two cycles, the variation of the flap deformation with time is shown in Fig. 6. The deformation during the open stage of the flexible valve is shown above the dotted line, and the deformation during the closed stage is shown below the dotted line. The deformation amount of the forward displacement reaches the maximum of 1.2 mm at 0.012 s, while the deformation amount of the reverse displacement reaches the maximum of 0.39 mm at 0.037 s. Significantly, the pressure causing the forward maximum deformation to be greater than the reverse maximum deformation is the same. Therefore, the FEM results prove that the forward direction of the flexible valve is easier to open than the reverse direction, and the deformation of the forward opening is greater than the reverse direction under the same loads.

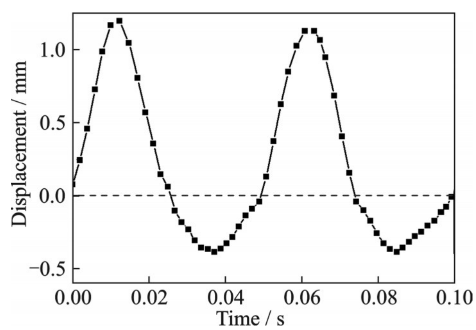

Fig.6 Relationship between flap deformation and time

Fig.7 shows the equivalent stress distribution of the flexible valve in the opening and closing process. The root of the flap has the highest equivalent stress, while the ventral flap has the lowest. In the repeated deformation process of the flexible valve, the local maximum stress is far less than the stress limit of the valve material, so there is no fatigue damage and the valve body is almost impossible to fail.

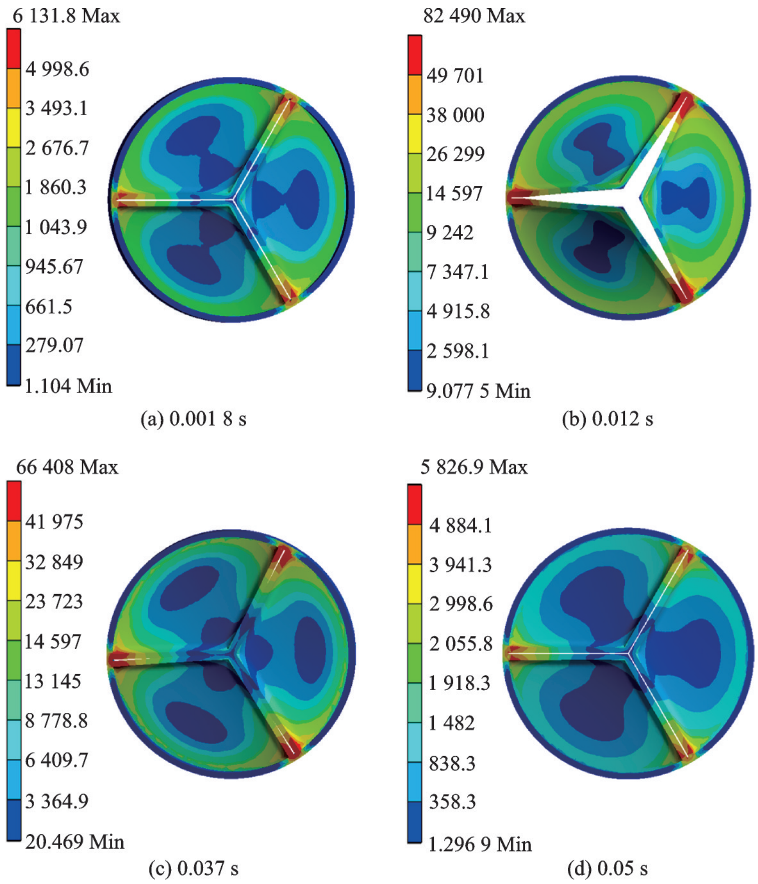

Fig.7 Equivalent stress distribution of flexible valve

3 Piezo-pumps Fabrication and Experiments

3.1 Prototype fabrication

Fig.8 shows a diagram of two different piezo-pumps with the diffuser/nozzle and cylinder. Both pump bodies are fabricated using stereolithography, and the packaging material is photosensitive resin (Godart 8118), as shown in Fig.9(a). The piezoelectric vibrator's structural parameters are described in Table 1[26]. Beryllium bronze has a diameter of 41 mm and a thickness of 0.15 mm, while piezoelectric ceramic has a diameter of 35 mm and a thickness of 0.12 mm. The piezoelectric pump with diffuser/nozzle has dimensions of 106 mm×56 mm×18 mm. The structural parameters of the diffuser/nozzle are determined as shown in Table 2. Table 3 lists the structural parameters of the piezo-

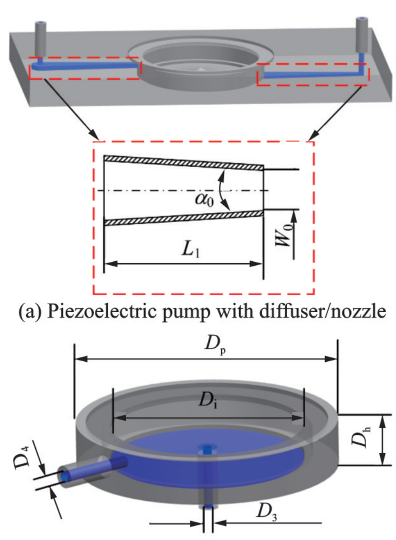

Fig.8 Schematic of piezoelectric pump with flexible valve

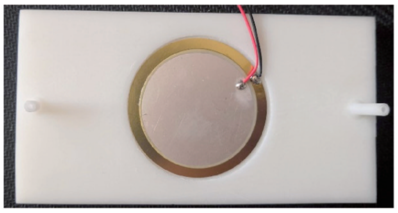

(a) Piezoelectric pump with diffuser/nozzle channels

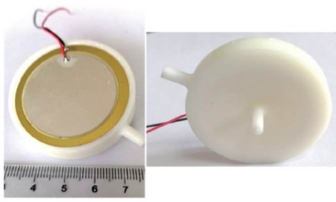

(b) Piezoelectric pump with cylinder channels

(c) Flexible valve

Fig.9 Prototype of two piezoelectric pumps and flexible valve

electric pump with cylinder tubes. The flexible valves are manufactured by 3D printing technology with the processing material of urethane resin. The diameter of the flexible valve is 36 mm and the height is 4 mm, as shown in Figs. 9 (b) and (c). The piezo-vibrator is bonded on the piezoelectric pump by silicone.

3.2 Cut-off performance of flexible valve

An experimental diagram of the cut-off performance of the flexible valve is shown in Fig.10. The fluid static pressure is used as the power source to test the cut-off performance of the flexible valve. The height difference of liquid level (ΔH) is changed by changing the pressure on the valve. The valve is placed in the sealed chamber. The inlet of the sealed chamber is connected to the jar. Electronic balance is used to weigh the mass flow from the outlet of sealed chamber. Deionized water is adopted as the liquid medium.

3.3 Output performance of piezoelectric pumps

The piezoelectric pumps used for testing include the cylinder piezoelectric pump with flexible valve (Pump 1), the diffuser/nozzle piezoelectric pump with flexible valve (Pump 2), and the valveless piezoelectric pump with diffuser/nozzle (Pump 3), respectively. Fig.11 shows the performance test of three pumps. The experimental voltage is 200 V (Peak-to-peak value), and the output flow of the piezoelectric pump per unit time is measured at different driving frequencies. The amplitude of the piezo-vibrator is measured by a laser displacement sensor (LK-G35, Keyence, Japan). The glycerol aqueous solutions with the concentration of 20% (Viscosity of 1.643 cP; 25 ℃), 30% (Viscosity of 2.157 cP; 25 ℃) and 40% (Viscosity of 3.281 cP, 25 ℃) are used to test the transfer capacity of the cylinder piezoelectric pump with flexible valve for certain-viscosity liquid.

Table 1 Material parameters of PZT vibrator

Material	Elastic matrix/GPa	Piezoelectricty / ($C\cdot m^{-2}$)	Permittivity/($F\cdot m^{-1}$)	Poisson's ratio	Density/ ($kg\cdot m^{-3}$)
Beryllium bronze	128			0.35	8 600
PZT-5A	$\begin{bmatrix} 12.1 & 7.54 & 7.52 & 0 & 0 & 0 \\ 7.54 & 12.1 & 7.52 & 0 & 0 & 0 \\ 7.52 & 7.52 & 11.1 & 0 & 0 & 0 \\ 0 & 0 & 0 & 2.11 & 0 & 0 \\ 0 & 0 & 0 & 0 & 2.11 & 0 \\ 0 & 0 & 0 & 0 & 0 & 2.26 \end{bmatrix} \times 10^{10}$	$\begin{bmatrix} 0 & 0 & -5.4 \\ 0 & 0 & -5.4 \\ 0 & 0 & 15.8 \\ 0 & 12.3 & 0 \\ 12.3 & 0 & 0 \\ 0 & 0 & 0 \end{bmatrix}$	$\begin{bmatrix} 8.107 & 0 & 0 \\ 0 & 8.107 & 0 \\ 0 & 0 & 7.346 \end{bmatrix} \times 10^{-9}$		7 750

Table 2 Structural parameters of channels

Parameter	Value
α_0/(°)	7
W_o/mm	1
L_1/mm	28.4
D_i/mm	34
D_P/mm	46
D_h/mm	7
$D_3=D_4$/mm	1

Table 3 η' of the maximum output flow rate

Pump	Frequency/Hz	Flow rate/ (mL·min^{-1})	Pressure/ Pa	Amplitude/μm	η'/N
1	10	15.382	519.2	72.9	18.259
2	10	5.682	676.7	73.9	8.672
3	7	2.206	196.1	57.7	0.875

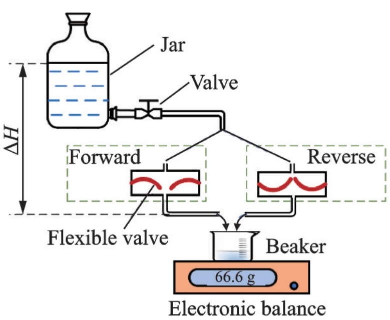

Fig.10 Experimental diagram of cut-off performance of flexible valve

4 Results and Discussion

Experimental results of the flexible valve are shown in Fig.12. The forward flow rate is significantly higher than the reverse when the pressure drop is increased, and the increase rate of the reverse velocity is much lower than that of the forward flow rate. When the pressure drop in forwarding flow reaches 88 Pa, the fluid overcomes the flow resistance and valve opening pressure, causing the fluid to flow out of the outlet. While in the reverse flow, 177 Pa pressure drop is required to overcome the flow resistance and valve opening resistance. Thus, the forward opening pressure of the flexible valve is less than the reverse-opening pressure, and it has certain reverse closure and linear control ability.

Fig.13 presents the experimental results of three pump output performances. The output flow of the three piezo-pumps is all increased firstly and then decreased with the increasing of the driving frequency. When the driving frequency is 10 Hz, Pump 1 and Pump 2 reach the maximum output flow of 15.38 mL/min and 5.68 mL/min, respectively. The maximum output flow of Pump 3 reaches 2.20 mL/min at 5 Hz. The output flow characteristics of Pump 1 are similar to those of Pump 2 at 5 Hz and 13 Hz. At 10 Hz, the maximum flow of Pump 1 is 9.7 mL/min, which is larger than Pump 2. The maximum flow rate of Pump 3 is much less than Pumps 1 and 2, as shown in Fig.13(a). The comparison between Pumps 2 and 3 indicates that the flexible valve can improve the flow resistance in the discharge and suction processes of the piezoelectric pump. Meanwhile, the flexible valve has the effect of improving the output flow rate. Compared with Pumps 1 and 2, the amplitude of the piezoelectric vibrator is similar at 10 Hz, as shown in Fig.13 (b). The flow rate of the cylinder piezoelectric

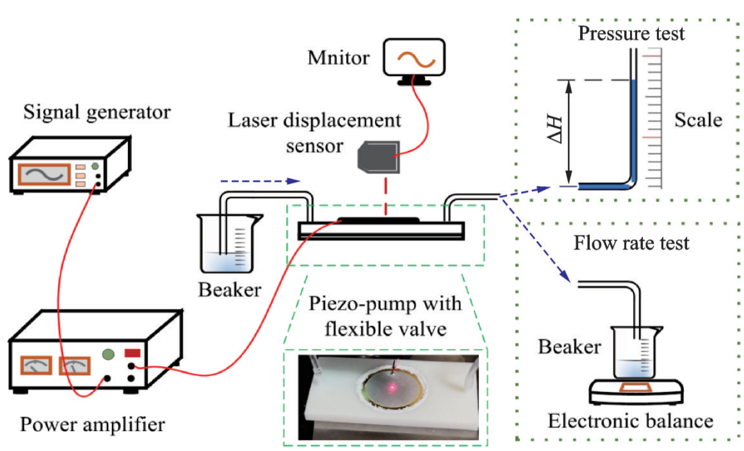

Fig.11 Schematic of experimental setup

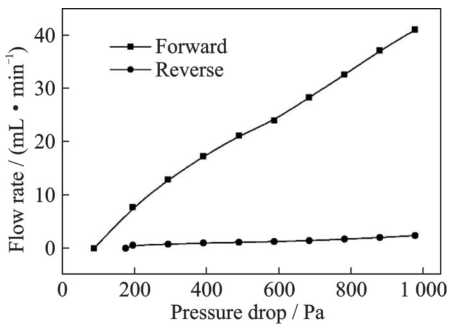

Fig.12 Forward and reverse flow rates under different pressure drops

pump with flexible valve (Pump 1) is 170.77% higher than that of the diffuser/nozzle piezoelectric pump with flexible valve (Pump 2).

Fig.13(b) presents the amplitude of the piezo-vibrator during the output performance tests. When the amplitude of the piezoelectric vibrator reaches the maximum value, the flow rate is not the maximum because of valve hysteresis. When the amplitude of the vibrator is maximum, the volume of the pump chamber changes the most. The hysteresis of the valve makes the fluid flow into the pump chamber less than the volume change. Fig.13(c) shows the back pressure with the driving frequency. When the driving frequencies of Pumps 1 and 2 are both 11 Hz, the output pressures reach the maximum values of 892.4 and 706.1 Pa, respectively. Fig. 13(d) shows the flow rate curves of piezo-pumps with different voltages, demonstrating that the output performance of piezo-pumps changes positively with the driving voltage increasing. By comparing the output performance of Pumps 2 and 3, it is shown that the flexible three flap valves have reverse cut-off features in the micropump, which improves the micropump's output performance. The output performance of Pump 1 is better than that of Pump 2 by changing the diffuser/nozzle channels to cylindrical channels.

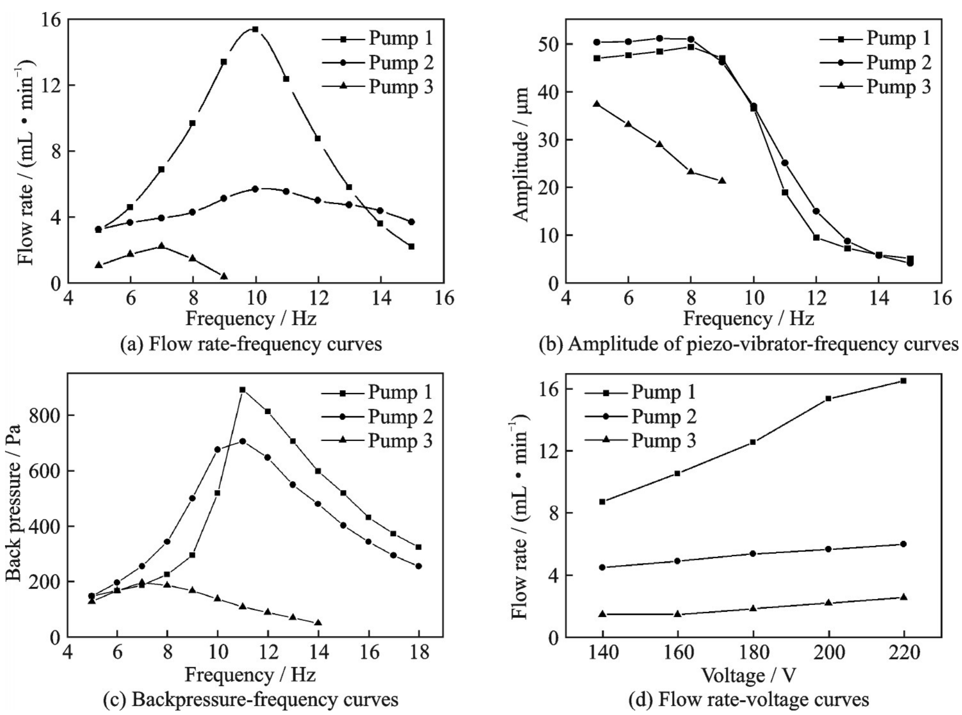

Fig.13 Experimental results of three pump output performances

To discuss why the output performance of Pump 1 is better than those of Pumps 2 and 3, the efficiency equation is proposed as

$$\eta = \frac{W_o}{W_i} \tag{3}$$

where W_i is the energy provided by the piezoelectric vibrator to the liquid per unit time, and W_o the energy of the fluid at the pump outlet per unit time.

On the one hand, the energy provided by the piezoelectric vibrator to the liquid per unit time (W_o) can be expressed as

$$W_o = PQ \tag{4}$$

On the other point, the energy of the fluid at the pump outlet per unit time (W_i) can be expressed as

$$W_i = fFD_f \tag{5}$$

where P is the output pressure, Q the output flow rate, f the driving frequency of the piezoelectric vibrator, D_f the maximum displacement of the center of the piezoelectric vibrator, and F the output force of the piezoelectric vibrator at the given frequency. Thus, Eq.(3) can be rewritten as

$$\eta = \frac{PQ}{FD_f f} \tag{6}$$

When the output force F is assumed all the same under the same conditions, Eq.(6) can be concluded as

$$\eta = \frac{1}{F} \times \frac{PQ}{D_f f} = \frac{1}{F}\eta' \tag{7}$$

$$\eta' = \frac{PQ}{D_f f} \tag{8}$$

where η' is defined as the output force of pumps, as shown in Tables 3 and 4.

Table 4 η' of the maximum output pressure

Pump	Frequency/Hz	Flow rate/ ($\text{mL}\cdot\text{min}^{-1}$)	Pressure/ Pa	Amplitude/μm	η'/N
1	11	12.37	892.4	37	54.698
2	11	5.548	706.1	50.1	14.335
3	7	2.206	196.1	57.7	0.875

From Tables 3 and 4, η' of Pump 1 is greater than those of Pumps 2 and 3, proving that Pump 1 is more efficient than Pumps 2 and 3, and it also explains why the output performance of Pump 1 is better than those of Pumps 2 and 3. Due to the better fluid transportability, the cylinder piezoelectric pump with flexible valve (Pump1) is adopted in the following viscosity experiments.

The relationship between the differential viscosity fluid and the output performance of the cylinder piezoelectric pump with flexible valve (Pump 1) is shown in Fig.14. The output flow rate and the output back pressure are affected by the liquid viscosity. The maximum flow rates at 1.643 cP, 2.157 cP, and 3.281 cP glycerols are 10.87, 6.94, and 1.3 mL/min, respectively. The maximum back pressure is 391.4, 369.6, and 313.7 Pa, respectively. With the increase of the viscosity, the maximum flow rate of the piezoelectric pump decreases, and the corresponding frequency of the maximum flow rate decreases gradually. It can be proved that the cylindrical piezo pump with flexible valve (Pump 1) can transmit a certain viscosity liquid.

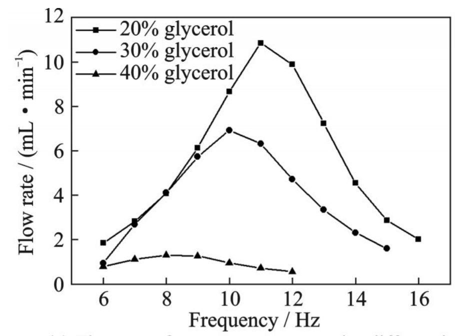

(a) Flow rate-frequency curves under differential viscosity fluid

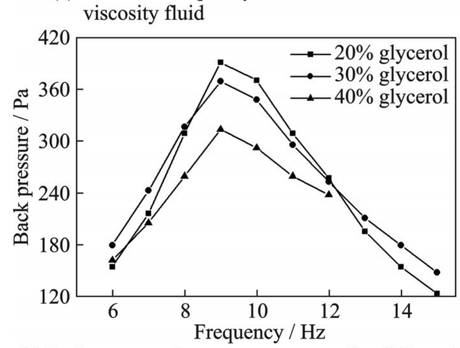

(b) Back pressure-frequency curves under differential viscosity fluid

Fig.14 Relationship between differential viscosity fluid and output performance of cylinder piezoelectric pump with flexible valve

5 Conclusions

A flexible arterial valve is proposed. The forward opening pressure of such a valve is less than its reverse-opening pressure, leading to a certain reverse closure ability and linear control ability of the proposed valve. The diffuser/nozzle piezoelectric pump with flexible valve and the cylinder piezoelectric pump with flexible valve are designed and manufactured, and a series of pump performance experiments are performed. The results indicate that the output performance of piezoelectric pumps with flexible valve is better than that of the valveless piezoelectric pump with diffuser/nozzle. The maximum flow rate of a cylinder piezoelectric pump with a flexible valve is 15.38 mL/min, 170.77% higher than the diffuser/nozzle piezoelectric pump with flexible valve. It is verified that the cylinder piezoelectric pump with flexible valve has high transmission efficiency. The glycerol aqueous solutions with the concentration of 20% and 40% are used as the transmission mediums, and the results indicate that the cylindrical piezo-pump with flexible valve can transmit a certain viscosity liquid. The piezoelectric pump with flexible valve has tremendous potential applications in the thermal control system of nanosats.

References

[1] HUNYADI G, GANLEY J, PEFFER A, et al. The university nanosat program: An adaptable, responsive and realistic capability demonstration vehicle[C]//Proceedings of 2004 IEEE Aerospace Conference. [S.l.]: IEEE, 2004.

[2] GARVEY J, BESNARD E. Development status of a nanosat launch vehicle[C]//Proceedings of the 40th AIAA/ASME/SAE/ASEE Joint Propulsion Conference and Exhibit. [S.l.]: AIAA, 2004: 4065.

[3] LEE D, VUKOVICH G, LEE R. Robust unscented Kalman filter for nanosat attitude estimation[J]. International Journal of Control, Automation and Systems, 2017, 15(5): 2161-2173.

[4] KING J T, KOLBECK J, KANG J S, et al. Performance analysis of nano-sat scale μCAT electric propulsion for 3U CubeSat attitude control[J]. Acta Astronautica, 2021,178: 722-732.

[5] BACCO M, CASSARÁ P, COLUCCI M, et al. A survey on network architectures and applications for nanosat and UAV swarms[C]//Proceedings of International Conference on Wireless and Satellite Systems. [S.l.]: Springer, 2017: 75-85.

[6] WOIAS P. Micropumps—Past, progress and future prospects[J]. Sensors and Actuators B: Chemical, 2005, 105(1): 28-38.

[7] ZHANG Che, ZHANG Renhui, LI Rennian, et al. Axial tip flow and performance analysis of squealer tip clearance for liquid ring pump blade[J]. Journal of Drainage and Irrigation Machinery Engineering, 2021, 39(4): 358-363. (in Chinese)

[8] SHI Guangtai, LIU Zongku, LI Helin, et al. Pressure fluctuation characteristics of gas-liquid two-phase flow in multiphase pump[J]. Journal of Drainage and Irrigation Machinery Engineering, 2021, 39(1): 23-29. (in Chinese)

[9] LEE K S, KIM B, SHANNON M A. An electrostatically driven valve-less peristaltic micropump with a stepwise chamber[J]. Sensors and Actuators A: Physical, 2012, 187: 183-189.

[10] PAN Q S, HE L G, HUANG F S, et al. Piezoelectric micropump using dual-frequency drive[J]. Sensors and Actuators A: Physical, 2015, 229: 86-93.

[11] DONG J S, LIU R G, LIU W S, et al. Design of a piezoelectric pump with dual vibrators[J]. Sensors and Actuators A: Physical, 2017, 257: 165-172.

[12] CHIA B T, LIAO H H, YANG Y J. A novel thermo-pneumatic peristaltic micropump with low temperature elevation on working fluid[J]. Sensors and Actuators A: Physical, 2011, 165(1): 86-93.

[13] EHSANI A, NEJAT A. Conceptual design and performance analysis of a novel flexible-valve micropump using magneto-fluid-solid interaction[J]. Smart Materials and Structures, 2017, 26(5): 055036.

[14] ROBERTSON J M, RODRIGUEZ R X, HOLMES L R, et al. Thermally driven microfluidic pumping via reversible shape memory polymers[J]. Smart Materials and Structures, 2016, 25(8): 085043.

[15] HUANG J, ZOU L, TIAN P, et al. Development of a valveless piezoelectric pump with vortex diodes[J]. Journal of Micromechanics and Microengineering, 2019, 29(12): 125006.

[16] HUANG J, ZOU L, TIAN P, et al. A valveless piezoelectric micropump based on projection micro litho stereo exposure technology[J]. IEEE Access, 2019, 7: 77340-77347.

[17] ZHANG J H, WANG Y, HUANG J. Advances in valveless piezoelectric pump with cone-shaped tubes[J]. Chinese Journal of Mechanical Engineering, 2017, 30(4): 766-781.

[18] FADL A, DEMMING S, ZHANG Z, et al. A multifunction and bidirectional valve-less rectification micropump based on bifurcation geometry[J]. Microfluidics and Nanofluidics, 2010, 9(2/3): 267-280.

[19] XIA Q X, ZHANG J H, LEI H, et al. Theoretical analysis and experimental verification on flow field of piezoelectric pump with unsymmetrical slopes element[J]. Chinese Journal of Mechanical Engineering, 2009, 22(5): 735-744.

[20] KAN J W, YANG Z G, PENG T J, et al. Design and test of a high-performance piezoelectric micropump for drug delivery[J]. Sensors and Actuators A:

Physical, 2005, 121(1): 156-161.

[21] YAMAHATA C, LACHARME F, BURRI Y, et al. A ball valve micropump in glass fabricated by powder blasting[J]. Sensors and Actuators B: Chemical, 2005, 110(1): 1-7.

[22] LEE S C, HUR S, KANG D, et al. The performance of bioinspired valveless piezoelectric micropump with respect to viscosity change[J]. Bioinspiration & Biomimetics, 2016, 11(3): 036006.

[23] PENG T J, GUO Q, YANG J, et al. A high-flow, self-filling piezoelectric pump driven by hybrid connected multiple chambers with umbrella-shaped valves[J]. Sensors and Actuators B: Chemical, 2019, 301(2): 126961.

[24] DONG J, CAO Y, CHEN Q, et al. Performance of single piezoelectric vibrator micropump with check valve[J]. Journal of Intelligent Material Systems and Structures, 2020, 31(1): 117-126.

[25] HUANG J, ZHU Y C, SHI W D, et al. Theory and experimental verification on cymbal-shaped slotted valve piezoelectric pump[J]. Chinese Journal of Mechanical Engineering, 2018, 31(1): 1-8.

[26] CUI Q, LIU C, ZHA X F. Study on a piezoelectric micropump for the controlled drug delivery system[J]. Microfluidics and Nanofluidics, 2007, 3(4): 377-390.

Acknowledgements This work was supported by the National Natural Science Foundation of China (Nos. 51605200, 61973207), the Natural Science Foundation of Shanghai (No.19ZR1474000), the Senior Talent Start-up Foundation of Jiangsu University (No.14JDG145), and the Foundation of State Key Laboratory of Mechanics and Control of Mechanical Structures of Nanjing University of Aeronautics and Astronautics (No.MCMS-E-0320G01).

Authors Mr. **LI Kai** received the M.S. degree in research center of fluid machinery engineering and technology, Jiangsu University in 2021. His research interests include design and simulation on piezoelectric micropumps.

Dr. **HUANG Jun** received the M.S. degree in nuclear technology and application and the Ph.D. degree in mechanical design and theory from Nanjing University of Aeronautics and Astronautics, respectively. Now he is an associate professor of research center of fluid machinery engineering and technology, Jiangsu University. His research interests include piezoelectric actuators and sensors.

Author contributions Dr. **HUANG Jun** provided ideas and revised the manuscript. Mr. **LI Kai** designed the models, wrote the manuscript, and contributed to data analysis. Mr. **LIU Jiaming** contributed to experimental methods and data. Dr. **ZHANG Quan** contributed to the discussion and revision of the study. Prof. **ZHANG Jianhui** contributed to the experiment analysis. Dr. **WANG Yuan** contributed to numerical simulation. All authors commented on the manuscript draft and approved the submission.

Competing interests The authors declare no competing interests.

(Production Editor: WANG Jing)

用于高黏度冷却液传输的柔性瓣膜阀压电泵

李 凯[1],刘家铭[2],张 泉[3],张建辉[4],黄 俊[2],王 渊[5]

(1.陕西空天动力研究院有限公司组合动力研发中心,西安 710003,中国;2.江苏大学流体机械工程技术研究中心,镇江 212013,中国;3.上海大学机电工程与自动化学院,上海 200072,中国;4.广州大学机械与电气工程学院,广州 510006,中国;5.陆军工程大学通信工程学院,南京 210007,中国)

摘要:为了输送纳卫星热控系统中的高黏度冷却液,提出了一种柔性瓣膜阀压电泵。根据人体主动脉瓣的形状特点设计了柔性瓣膜阀的结构,旨在模拟人体心脏的仿生泵送功能。通过有限元的方法对柔性瓣膜阀进行了应力-应变分析,结果表明柔性阀具有单向截止性并可集成于压电微泵。开发并加工制作了锥形管柔性瓣膜阀压电泵和柱形管柔性瓣膜阀压电泵,输出性能试验结果表明,柱形管柔性阀压电泵的最大流量为15.38 mL/min,比锥形管柔性阀压电泵的流量高170.77%。试验验证了柱形管柔性阀压电泵具有输送高黏度液体的能力,在纳卫星热控制系统中具有应用潜力。

关键词:压电泵;高黏度液体;柔性阀;截止性能;输出特性